Effect of Variations in the Structure of a Polyleucine-Based α-Helical Transmembrane Peptide on Its Interaction with Phosphatidylcholine Bilayers†

Feng Liu, Ruthven N. A. H. Lewis, Robert S. Hodges, and Ronald N. McElhaney*

Department of Biochemistry, University of Alberta, Edmonton, Alberta, Canada T6G 2H7

Received February 11, 2002; Revised Manuscript Received May 2, 2002

ABSTRACT: High-sensitivity differential scanning calorimetry (DSC) and Fourier transform infrared (FTIR) spectroscopy were used to study the interaction of an α-helical transmembrane peptide, acetyl-Lys_2-Leu_{24}-Lys_2-amide (L_{24}), and odd-chain members of the homologous series of *n*-saturated diacylphosphatidylcholines. An analogue of L_{24}, in which the lysine residues were all replaced by 2,3-diaminopropionic acid, and another, in which a leucine residue at each end of the polyLeu sequence was replaced by a tryptophan, were also studied. At low peptide concentrations, the DSC thermograms exhibited by these lipid/peptide mixtures are resolvable into two components. One of these components is fairly narrow, highly cooperative, and exhibits properties which are similar to but not identical with those of the pure lipid. In addition, the transition temperature and cooperativity of this component, and its fractional contribution to the total enthalpy change, decrease with an increase in peptide concentration, more or less independently of phospholipid acyl chain length. The other component is very broad and predominates at high peptide concentrations. These two components have been assigned to the chain-melting phase transitions of populations of peptide-poor and peptide-enriched lipid domains, respectively. Moreover, when the mean hydrophobic thickness of the PC bilayer is less than the peptide hydrophobic length, the peptide-associated lipid melts at higher temperatures than does the bulk lipid and vice versa. In addition, the chain-melting enthalpy of the broad endotherm does not decrease to zero even at high peptide concentrations, suggesting that these peptides reduce somewhat but do not abolish the cooperative gel/liquid-crystalline phase transition of the lipids with which it is in contact. Our DSC results indicate that the width of the broad phase transition observed at high peptide concentration is inversely but discontinuously related to hydrocarbon chain length. Our FTIR spectroscopic data indicate that these peptides form a very stable α-helix under all of our experimental conditions but that small distortions of their α-helical conformation are induced in response to mismatch between peptide hydrophobic length and gel-state bilayer hydrophobic thickness. We also present evidence that these distortions are localized to the N- and C-terminal regions of these peptides. Interestingly, replacing the terminal Lys residues of L_{24} by 2,3-diaminopropionic acid residues actually attenuates the hydrophobic mismatch effects of the peptide on the thermotropic phase behavior of the host PC bilayer, in contrast to the predictions of the snorkel hypothesis. We rationalize this attenuated hydrophobic mismatch effect by postulating that the 2,3-diaminopropionic acid residues are too short to engage in significant electrostatic and hydrogen-bonding interactions with the polar headgroups of the host phospholipid bilayer, even in the absence of any hydrophobic mismatch between incorporated peptide and the bilayer. Similarly, the reduced hydrophobic mismatch effect also observed when the two terminal Leu residues of L_{24} are replaced by Trp residues is rationalized by considering the lower energetic cost of exposing the Trp as opposed to the Leu residues to the aqueous phase in thin PC bilayers and the higher cost of inserting the Trp as opposed to the Leu residues into the hydrophobic cores of thick PC bilayers.

The mutual interactions of lipids and proteins are fundamentally important to both the structure and the function of all biological membranes (*1*, *2*). In particular, the chemical composition and physical properties of the host lipid bilayer can markedly influence the activity and thermal stability of a large number of integral membrane proteins in both model and biological membrane systems (*1*−*5*). For this reason, there have been many studies of the interactions of membrane proteins with their host lipid bilayers, in both biological and reconstituted model membrane systems, employing a wide range of different physical techniques (*6*−*10*). However, our understanding of the physical principles underlying lipid/protein interactions remains incomplete, and the actual molecular mechanisms whereby associated lipids actually alter the activity, and presumably also the structure and dynamics, of integral membrane proteins are largely unknown. This situation is due in part to the fact that most transmembrane proteins are relatively large, multidomain

† Supported by operating and major equipment grants from the Canadian Institutes of Health Research (R.N.M.) and major equipment grants from the Alberta Heritage Foundation for Medical Research (R.N.M.).

* Corresponding author. Telephone: (780) 492-2413. Fax: (780) 492-0095. E-mail: rmcelhan@gpu.srv.ualberta.ca.

10.1021/bi025661i CCC: $22.00
Published on Web 06/27/2002

macromolecules of complex and often unknown three-dimensional structure and topology that can interact with lipid bilayers in complex, multifaceted ways (*1*−*10*). To overcome this problem, a number of workers have designed and synthesized peptide models of specific regions of natural membrane proteins and have studied their interactions with model lipid membranes of defined composition (*11*, *12*). Physical studies of such relatively tractable model membrane systems have already significantly advanced our understanding of the molecular basis of lipid/protein interactions.

The synthetic peptide acetyl-K_2-G-L_{24}-K_2-A-amide (P_{24})[1] and its analogues have been successfully utilized as a model of the hydrophobic transmembrane α-helical segments of integral membrane proteins (*12*, *13*). These peptides contain a long sequence of hydrophobic leucine residues capped at both the N- and C-termini with two positively charged, relatively polar lysine residues. Moreover, the normally positively charged N-terminus and the negatively charged C-terminus have both been blocked to provide a symmetrical tetracationic peptide that will more faithfully mimic the transbilayer region of natural membrane proteins. The central polyleucine region of these peptides was designed to form a maximally stable α-helix, particularly in the hydrophobic environment of the lipid bilayer core, while the dilysine caps were designed to anchor the ends of these peptides to the polar surface of the lipid bilayer and to inhibit the lateral aggregation of these peptides. In fact, CD (*13*) and FTIR (*14*−*16*) spectroscopic studies of P_{24} have shown that it adopts a very stable α-helical conformation both in solution and in lipid bilayers, and X-ray diffraction (*17*), fluorescence quenching (*18*), and FTIR spectroscopic (*14*−*16*) studies have confirmed that P_{24} and its analogues assume a transbilayer orientation with the N- and C-termini exposed to the aqueous environment and the hydrophobic polyleucine core embedded in the hydrocarbon core of the lipid bilayer when reconstituted with various PCs. DSC (*13*, *15*, *19*−*21*) and ^{2}H NMR spectroscopic (*13*, *19*, *20*) studies have shown that P_{24} broadens the gel/liquid-crystalline phase transition and reduces its enthalpy. The phase transition temperature is shifted either upward or downward, depending on the degree of mismatch between the hydrophobic length of the peptide and the hydrophobic thickness of PC lipid bilayers (*15*), but this is not observed in PE bilayers, where P_{24} substantially decreases the phase transition temperature in a hydrocarbon chain length-independent manner (*21*). Moreover, in both P_{24}/PC and P_{24}/PE systems, the hydrocarbon chains of the phospholipids alter their conformation to accommodate any hydrophobic mismatch with the incorporated peptide (*15*, *21*). As well, small distortions of the α-helical conformation of P_{24} are also observed in response to peptide/lipid hydrophobic mismatch (*15*). ^{2}H NMR (*22*) and ESR (*23*) spectroscopic studies have shown that the rotational diffusion of P_{24} about its long axis perpendicular to the membrane plane is rapid in the liquid-crystalline state of the bilayer and that the closely related peptide L_{24} exists at least primarily as a monomer in liquid-crystalline POPC bilayers, even at relatively high peptide concentrations.

A similarly designed peptide, $(LA)_{12}$, in which the polyleucine core of L_{24} is replaced by alternating leucine and alanine residues, has also been investigated to examine whether the replacement of one-half of the leucine residues by smaller and less hydrophobic alanine residues would influence the stability of the helical form of the peptide and if the surface topology of a transmembrane peptide would alter its effects on lipid bilayers. The application of a variety of physical techniques has revealed that the behavior of $(LA)_{12}$ in solution and in lipid micelles or bilayers is generally similar to that of P_{24} (*24*−*26*). However, $(LA)_{12}$ perturbs the gel/liquid-crystalline phase transition of PC and PE bilayers to a greater extent than does P_{24} at comparable concentrations, as inferred from the greater decrease of the temperature and enthalpy of the gel/liquid-crystalline phase transition, possibly due partly to its rougher surface topology. However, the influence of the hydrophobic mismatch between the peptide and the host PC bilayer on the shift in the phase transition temperature is less pronounced for $(LA)_{12}$ than for L_{24}, perhaps due in part to the greater conformational plasticity of $(LA)_{12}$ in response to alterations of the bilayer thickness (*25*, *26*). Finally, we have recently shown that the related polyalanine-based peptide A_{24} is insufficiently hydrophobic to assume an α-helical transmembrane orientation in hydrated PC bilayers (*27*).

In this study, we investigate the effects of the α-helical transmembrane peptide L_{24} and the structurally related peptides L_{24}-DAP and W-L_{22}W on the thermotropic phase behavior of four odd-chain PC bilayers of differing hydrocarbon chain lengths. These structural derivatives of L_{24} were used to evaluate several hypotheses related to the effects of peptide/lipid hydrophobic mismatch on the thermotropic phase behavior of phospholipid model membranes. First, with the peptide L_{24}-DAP, the two pairs of capping lysine residues at the terminus of L_{24} have been replaced with the lysine analogues of DAP, in which three of the four side-chain methylene groups have been removed. This peptide was used to test the so-called snorkel model first suggested by Segrest et al. (*28*) to explain the behavior of positively charged residues in the amphipathic helixes present at the surfaces of blood lipoproteins and later extended to transmembrane α-helices by von Heijne et al. (*29*). According to the transmembrane peptide version of the snorkel model, the long, flexible hydrophobic side chains of lysine or arginine can extend along the transmembrane helix so that the terminal charged moiety can reside in the lipid polar headgroup region while the α-carbon of the amino acid residue remains well below (or possibly above) the membrane−water interface, even when the hydrophobic length of the peptide is considerably different from that of the host lipid bilayer. Because of the shorter spacer arms between the charged group and the α-carbon of DAP, the peptide L_{24}-DAP is expected to be less accommodating to hydrophobic mismatch, and any effects of such mismatch on the thermotropic phase behavior of its host lipid bilayer should be exaggerated.

Second, to investigate the importance of interfacially located tryptophan residues with respect to the effects of transmembrane peptides on their host lipid bilayer, we have

[1] Abbreviations: P_{24}, acetyl-Lys_2-Gly-Leu_{24}-Lys_2-Ala-amide; L_{24}, acetyl-Lys_2-Leu_{24}-Lys_2-amide; L_{24}-DAP, acetyl-DAP_2-Leu_{24}-DAP_2-amide; W-L_{22}-W, acetyl-Lys_2-Trp-Leu_{22}-Trp-Lys_2-amide; DAP, 2,3-diaminopropionic acid; PC, phosphatidylcholine, where the number before the colon represents the total number of carbon atoms in the hydrocarbon chains and the number after the colon the number of double bonds; DSC, differential scanning calorimetry; FTIR, Fourier transform infrared; ESR, electron spin resonance; NMR, nuclear magnetic resonance; $L_{\beta'}$, lamellar gel phase with tilted hydrocarbon chains; L_α, lamellar liquid-crystalline phase.

also examined the effect of the peptide W-L_{22}-W on the thermotropic phase behavior of PC model membranes. W-L_{22}-W is an L_{24} derivative in which residues Leu-3 and Leu-26 are replaced with tryptophans. The preference of tryptophan and tyrosine residues for the polar−apolar interfaces of the membrane lipid bilayer is found to be one of the common features of natural membrane proteins (*30*−*32*).

MATERIALS AND METHODS

The phospholipids used in this study were obtained from Avanti Polar Lipids Inc. (Alabaster, AL) and were used without further purification. Commercially supplied solvents of at least analytical grade quality were redistilled prior to use. Peptides were synthesized and purified as trifluoroacetate salts using previously published solid-phase synthesis and reversed-phase high-performance liquid chromatographic procedures (*24*).

Samples were prepared for DSC as follows. Lipid and peptide were codissolved in methanol to attain the desired lipid-to-peptide ratio, and the solvent was removed with a stream of nitrogen, leaving a thin film on the sides of a clean glass test tube. This film was subsequently dried in vacuo for several hours to ensure removal of the last traces of solvent. Samples containing 0.5−0.8 mg of lipid were then hydrated by vigorous vortexing with a buffer (50 mM Tris, 150 mM NaCl, 1mM NaN_3, pH 7.4) at temperatures some 10−15 °C above the gel/liquid-crystalline phase transition temperature of the lipid. DSC thermograms were obtained from 0.5 mL samples with a high-sensitivity Microcal VP-DSC instrument (Microcal Inc., Northampton MA), operating at heating and cooling rates of 10 °C/h. The data were analyzed and plotted with the Origin software package (OriginLab Corp., Northampton, MA).

Peptide samples to be used in FTIR spectroscopic experiments were converted to the hydrochloride salt by two cycles of lyophilization from 10 mM hydrochloric acid. This procedure was necessary because the trifluoroacetate ion gives rise to a strong absorption band (~1670 cm^{-1}) which partially overlaps the amide I absorption band of the peptide (*15*). Typically, samples were prepared by codissolving lipid and peptide in methanol at lipid-to-peptide molar ratios near 30:1. After removal of the solvent and drying of the film (see above), samples containing 2−3 mg of lipid were hydrated by vigorous mixing with 75 μL of a D_2O-based buffer (50 mM Tris, 150 mM NaCl, 1 mM NaN_3, pD 7.4). The aqueous suspension obtained was then squeezed between the CaF_2 windows of a heatable, demountable liquid cell (NSG Precision Cells, Farmingdale, NY) equipped with a 25 μm Teflon spacer. Once the cell was mounted in the sample holder of the spectrometer, the sample temperature could be varied between 20 and 90 °C by an external, computer-controlled water bath. Infrared spectra were acquired as a function of temperature with a Digilab FTS-40 Fourier transform spectrometer (Bio-Rad, Digilab Division, Cambridge, MA) using data acquisition parameters similar to those described by Mantsch et al. (*33*). The experiment involved a sequential series of 2 °C temperature ramps with a 20 min interramp delay for thermal equilibration and was equivalent to a scanning rate of 4 °C/ h. Spectra were analyzed with software supplied by the instrument manufacturers and other programs obtained from the National Research Council of Canada.

Table 1: Hydrophobic Thickness of Bilayers Formed by Various Phosphatidylcholines

	hydrophobic thickness (Å)[a]		
PC	gel phase	liquid-crystalline phase	mean[b]
13:0	31.5	21.0	26.3
15:0	36.8	24.5	30.7
17:0	42.0	28.0	35.0
19:0	47.2	31.5	39.4

[a] Hydrophobic thicknesses were calculated as in Zhang (*15*). [b] The mean of the hydrophobic thickness of the gel and liquid-crystalline phases.

RESULTS

To investigate the effects of hydrophobic mismatch between the three peptides studied here and the host lipid bilayer, we utilized four odd-chain linear saturated PCs ranging in chain length from 13 to 19 carbon atoms in the present study. There were several reasons for this choice of phospholipids. First, our previous studies of the closely related peptide P_{24} indicated that this peptide exhibits reduced solubility in PCs containing 12 or fewer or 20 or more carbon atoms but is soluble to levels of at least 10 mol % in PCs containing 13−19 carbon atoms (*14*, *15*). Second, these studies revealed that the best match of peptide effective hydrophobic length and phospholipid mean hydrophobic thickness (see below) occurred for 15:0 PC (*14*, *15*). Third, since we are utilizing three different peptides in the present study rather than a single peptide as in our previous work, there was a need to reduce the total number of peptide/PC systems examined. We thus chose to utilize only odd-chain PCs containing 13−19 carbon atoms in the present investigation, since this choice allowed us to cover the maximum range of lipid bilayer thicknesses compatible with high peptide incorporation. Since our previous work with P_{24} also demonstrated that the effects of this peptide on phospholipid thermotropic phase behavior varies regularly and monotonically with variations in hydrocarbon chain length (*15*, *21*), restricting our studies to the odd-chain PCs should not significantly reduce the value of this study while saving considerable time and effort.

The four odd-chain PCs utilized here, and their hydrophobic thicknesses in both the gel and liquid-crystalline states, are shown in Table 1. These values of bilayer hydrophobic thicknesses can be compared with the effective hydrophobic length of the polyleucine sequence of L_{24}, which we calculate to be 30.6 Å, assuming that this peptide adopts an ideal α-helical conformation when incorporated into phospholipid bilayers. Note that the effective hydrophobic length of L_{24} of 30.6 Å is defined here as the average length of the polyleucine α-helix as measured at any point on its surface in a direction parallel to the helical axis and is smaller than the 36.0 Å end-to-end distance of a stretch of 24 leucine residues (see ref *15*). Given this value, note that the effective hydrophobic length of L_{24} and its analogues approximately matches the hydrophobic thickness of 13:0 PC bilayers in the gel state but is progressively shorter than the hydrophobic thickness of gel-state bilayers composed of the longer chain

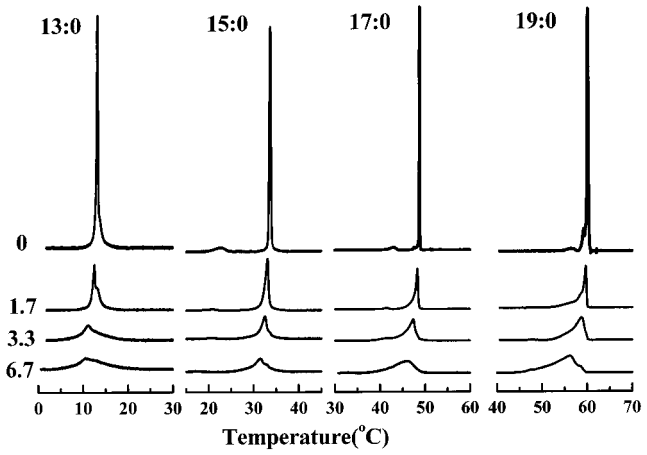

FIGURE 1: Effect of L_{24} on the DSC heating thermograms of a series of *n*-saturated diacyl-PCs varying in hydrocarbon chain length. The mole percent of peptide present in each sample is indicated in the column of numbers printed on the left side of the figure.

PCs studied here. Similarly, peptide effective length will approximately match the hydrophobic thickness of 19:0 PC bilayers in the liquid-crystalline state but will progressively exceed the hydrophobic thicknesses of the shorter chain liquid-crystalline PC bilayers. Finally, note that the mean hydrophobic thickness of 15:0 PC bilayers is very close to the calculated effective hydrophobic length of L_{24} and its analogues. Thus a mismatch between peptide hydrophobic length and mean bilayer hydrophobic thickness will occur with both the shorter and longer chain PCs studied here.

We stress that the pattern of hydrophobic mismatch described above strictly applies only if the conformation of L_{24} and its analogues is not altered by changes in host bilayer thickness and conversely that the presence of these peptides does not significantly alter the conformation of the phospholipid hydrocarbon chains of the host PC bilayer. However, our previous DSC and FTIR spectroscopic studies of P_{24} (*15*, *21*), and the present studies of L_{24} (see below), suggest that even these strongly α-helical polyleucine-based peptides can alter the pitch of their helices in response to variations in host bilayer thicknesses, at least in gel-state bilayers. Conversely, the hydrocarbon chains of PC and PE bilayers can also change their degree of conformational order, and thus their effective hydrophobic thicknesses, to accommodate to the presence of these model peptides (*15*, *21*). Moreover, this previous work and our recent ESR (*23*) and ^{2}H NMR (*34*) studies indicate that these peptides intrinsically disorder gel and order liquid-crystalline PC bilayers, even when hydrophobic mismatch effects are taken into consideration. Also, when the hydrophobic length of the peptide significantly exceeds that of the hydrophobic thickness of the liquid-crystalline host bilayer, peptide tilt may occur (see refs *11* and *12*). Thus, the actual degree of hydrophobic mismatch between L_{24} and its analogues and the host PC bilayers studied here may be less than that indicated by the data presented in Table 1, which is for PC bilayers in the absence of peptide.

Thermotropic Phase Behavior of Phosphatidylcholine Bilayers in the Absence of Peptide. As illustrated in Figure 1, in the absence of peptide the four odd-chain saturated PCs studied here by DSC exhibit a lower temperature, lower enthalpy, less cooperative pretransition and a higher temperature, higher enthalpy, more cooperative main transition upon heating. The pretransition arises from the conversion of the lamellar gel ($L_{\beta'}$) phase to the lamellar rippled gel ($P_{\beta'}$) phase and the main phase transition from the conversion of the $P_{\beta'}$ to the lamellar liquid-crystalline (L_α) phase. The midpoint temperature of both the pretransition and main phase transition increases with increases in the length of the PC hydrocarbon chains. However, the pretransition exhibits a steeper dependence on fatty acyl chain length than does the main transition, so that the temperature interval between these two phase transitions decreases as hydrocarbon chain length increases. The 13:0 PC (and 12:0 PC) are unique in the homologous series of linear saturated PCs in exhibiting a high temperature shoulder on the main phase transition endotherm. Although the physical basis of this unusual behavior is not fully understood, both thermal events are known to involve phospholipid hydrocarbon chain melting (*35*, *36*) and will thus be considered as $P_{\beta'}/L_\alpha$ phase transitions in the analysis presented below. The reader is referred to Lewis et al. (*36*) and references therein for a more thorough discussion of the thermotropic phase behavior of the entire homologous series of linear saturated PCs.

Effect of Peptide Incorporation on the Pretransition. The effect of the incorporation of L_{24} and its analogues on the pretransition of 13:0 PC could not be determined by DSC as the pretransition temperature of −1 °C overlaps with the ice-melting endotherm centered near 0 °C. However, the incorporation of increasing quantities of peptide into the longer chain PC bilayers lowers the temperature, enthalpy, and cooperativity of the pretransition in each case, abolishing it entirely at a peptide incorporation levels above 6.7 mol % (see Figure 1). These results suggest that the presence of L_{24} reduces and eventually abolishes hydrocarbon chain tilt in these gel phase bilayers, causing the progressive replacement of the $L_{\beta'}$ and $P_{\beta'}$ phases with a disordered L_β-like phase (*15*, *25*). Interestingly, the incorporation of peptide is more effective in this regard in the shorter chain PC bilayers where the hydrophobic mismatch between peptide hydrophobic length and bilayer hydrophobic thickness in the gel phase is minimal. Essentially identical results were found for the L_{24} analogues L_{24}-DAP and W-L_{22}-W.

Effect of Peptide Incorporation on the Main Transition. The effect of the incorporation of L_{24} on the main phase transition of the four PCs studied here is also illustrated in Figure 1. In all cases the incorporation of increasing quantities of peptide produces a two-component DSC endotherm (in the case of 13:0 PC, a three-component endotherm; see Figure 2), as well as a progressive decrease in the enthalpy and cooperativity of the overall gel to liquid-crystalline phase transition of the host PC bilayer. The relative contribution of the sharp component of the DSC endotherm, which initially possesses a phase transition temperature, enthalpy, and cooperativity relatively similar to that of the PC alone, decreases in magnitude as the proportion of L_{24} increases, and this component vanishes entirely at an L_{24} content of 6.7 mol %. In contrast, the relative contribution of the broad component increases as the peptide concentration increases, and it is the only component which persists at the highest peptide concentration tested. Using the rationale provided in our previous DSC studies of the interaction of P_{24} and related peptides with lipid bilayers (*15*, *21*, *25*, *26*), we assign the sharp component

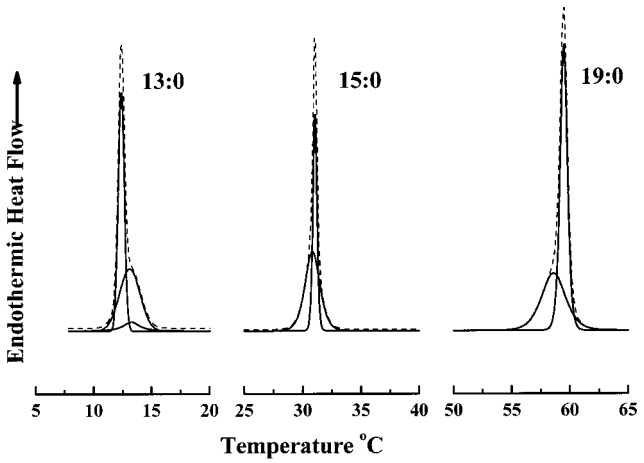

FIGURE 2: Illustration of the results of the curve-fitting procedure used to resolve the components of the DSC heating thermograms exhibited by mixtures of L_{24} with PC bilayers. The examples shown are L_{24}/13:0 PC (left panel), L_{24}/15:0 PC (middle panel), and L_{24}/19:0 PC (right panel). In all cases the samples contained 3.3 mol % of L_{24}.

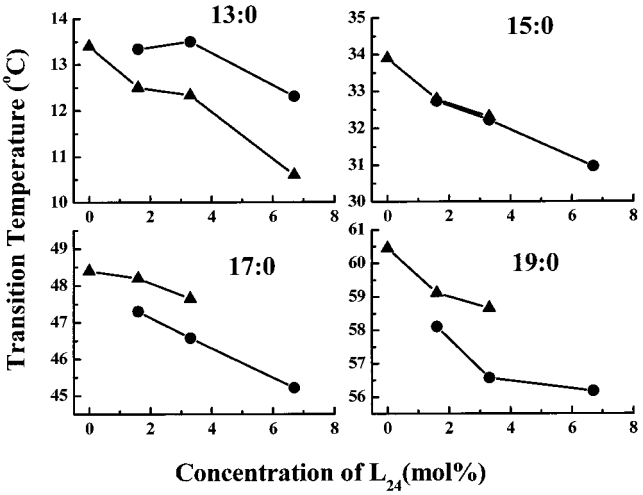

FIGURE 3: Effect of L_{24} concentration on the peak temperature of the two components of the DSC thermograms exhibited by the mixtures of L_{24} and the *n*-saturated diacyl-PCs studied. The symbols (▲) and (●) represent the sharp and broad components of the DSC endotherms, respectively.

of our DSC endotherms to the hydrocarbon chain-melting phase transition of peptide-poor PC domains and the broad component to the melting of peptide-rich PC domains. Moreover, we ascribe the small decrease in the temperature and cooperativity of the sharp component of the DSC endotherms to domain boundary effects arising from the decreasing size of the peptide-poor PC domains, which of course also explains their progressively smaller enthalpy as peptide concentration increases. Note that these characteristic effects of L_{24} and its analogues on the sharp component are noted in all the PCs studied and are hydrocarbon chain length independent.

In contrast to the PC hydrocarbon chain length-independent effects of L_{24} incorporation on the temperature, enthalpy, and cooperativity of the sharp component of the DSC endotherm, the effects of peptide incorporation on the thermodynamic parameters of the broad component depend on the hydrocarbon chain length and thus on the thickness of the host PC bilayer. For example, as illustrated in Figure 3, the phase transition temperature of the broad component of the DSC endotherm occurs at a higher temperature than that of the sharp component in 13:0 PC bilayers, at the same temperature in 15:0 PC bilayers, but at lower temperatures in 17:0 and 19:0 PC bilayers, although in all cases the phase transition temperatures of both components decrease with increasing peptide concentration. This result is predicted by hydrophobic mismatch theory, since the effective hydrophobic length of L_{24} is greater, matches, and is less than the mean hydrophobic thickness of 13:0 PC, 15:0 PC, and 17:0 or 19:0 PC bilayers, respectively (*37*−*39*).

A comparison of the effects of a mismatch between peptide hydrophobic length and PC bilayer hydrophobic thickness on the magnitude of the shift of the phase transition temperature of the broad component of the phospholipid phase transition is presented in Figure 4. Although the characteristic hydrophobic mismatch-dependent shift in phase transition temperature discussed above for L_{24} is also observed for the two L_{24} analogues, the magnitude of this shift is considerably attenuated for W-L_{22}-W and especially for L_{24}-DAP. This result suggests that these two peptides

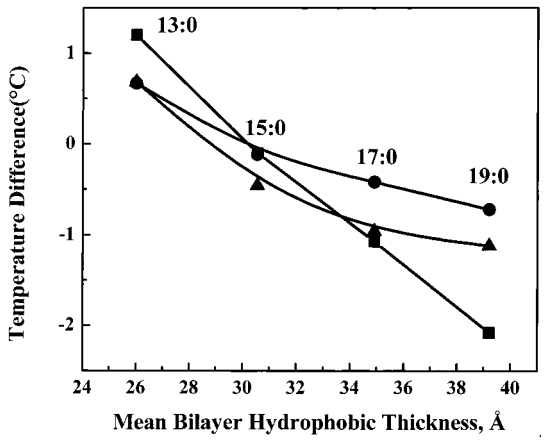

FIGURE 4: Plot of the differences of the transition temperatures of the peptide-associated and the bulk lipids versus the mean hydrophobic thickness of the lipid bilayer at a peptide concentration of 3.3 mol %. The symbols (■), (●), and (▲) represent peptides L_{24}, L_{24}-DAP, and W-L_{22}-W, respectively.

are better able to accommodate to alterations in the hydrophobic thickness of the host PC bilayer than can L_{24} itself. We note here, however, that the snorkel hypothesis would predict that the hydrophobic mismatch effect on the phase transition temperature of the host lipid bilayer would be *greater* for L_{24} DAP than for L_{24} itself, in contrast to the results presented above.

A hydrocarbon chain length-dependent effect was also noted for the dependence of the overall phase transition enthalpy on L_{24} concentration (see Figure 5). Although in all cases the overall phase transition enthalpy decreases with increasing peptide concentration, the rate of decrease in enthalpy is greatest for the shortest chain PC and decreases as the hydrocarbon chain length increases. Thus both the absolute and relative decreases in overall transition enthalpy are largest for 13:0 PC and smallest for 19:0 PC bilayers. However, the progressive but nonlinear decrease in the transition enthalpy of the sharp component and the corresponding increase in the transition enthalpy of the broad component are more or less comparable in each peptide/PC mixture examined. Note that an appreciable phase transition

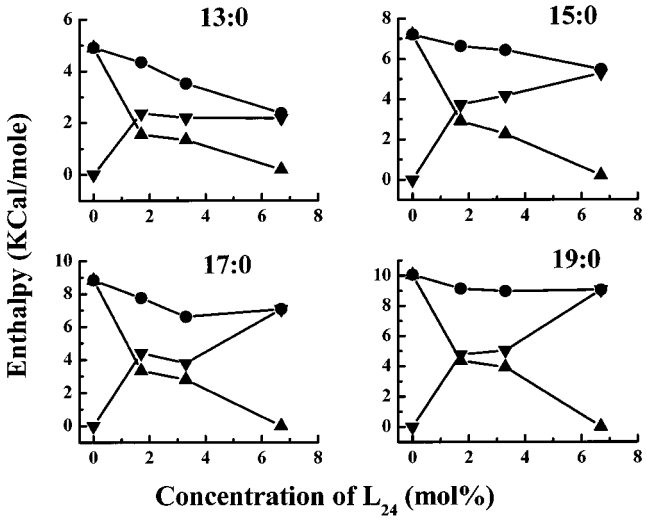

FIGURE 5: Effect of L_{24} concentration on the transition enthalpies of the two components of the DSC thermograms exhibited by mixtures of peptides and *n*-saturated diacyl-PCs. The symbols (●), (▲), and (▼) represent the total enthalpy and the enthalpy of the sharp and broad components of the DSC endotherms, respectively.

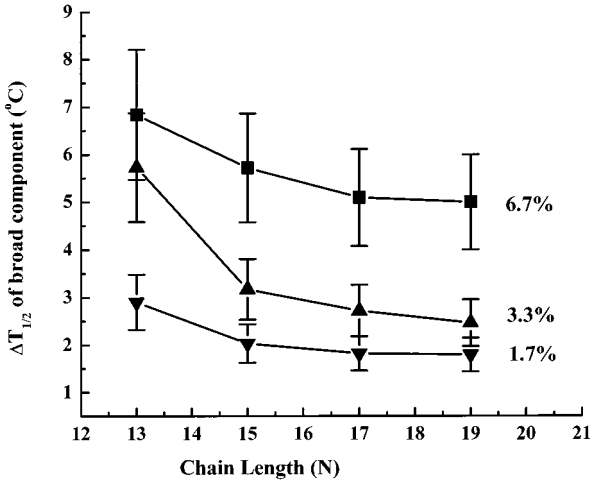

FIGURE 6: Effect of L_{24} concentration on the cooperativity ($\Delta T_{1/2}$) of the broad component of the DSC thermograms of the various PCs studied. The symbols (▼), (▲), and (■) represent peptide concentrations of 1.7, 3.3, and 6.7 mol %, respectively.

enthalpy remains even at relatively high peptide concentrations where the sharp transition due to the melting of peptide-poor PC domains has completely disappeared. This result indicates that the presence of even high concentrations of L_{24} modestly reduces the magnitude of the cooperative gel to liquid-crystalline phase transition of the host lipid bilayers but certainly does not abolish it entirely, as also indicated by the FTIR spectroscopic results to be presented below. The same relationship between phase transition enthalpy and peptide concentration observed for L_{24} was also observed for the L_{24} analogues L_{24}-DAP and W-L_{22}-W.

The effect of L_{24} concentration on the cooperativity of the broad component of the gel/liquid-crystalline phase transition is also dependent on the hydrocarbon chain length of the host PC bilayer, as illustrated in Figure 6. Although in all cases the width of the phase transition increases with increases in the concentration of the peptide, this decrease in cooperativity is greatest for the shorter hydrocarbon chain length PC bilayers, where the peptide hydrophobic length

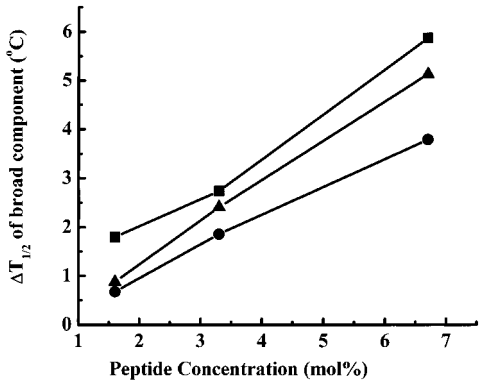

FIGURE 7: Comparison of the effects of variations in the concentration of L_{24}(■), L_{24}-DAP (●), and W-L_{22}-W (▲) on the cooperativity ($\Delta T_{1/2}$) of the broad component of the DSC thermograms in the mixtures of peptide and 17:0 PC.

and the hydrophobic thickness of the gel-state bilayer are most closely matched. The possible molecular basis for this effect will be discussed later.

The effect of increasing concentrations of each of the three peptides studied here on the cooperativity of the broad component of the phase transition of 17:0 PC bilayers is presented in Figure 7. Although the cooperativity of this chain-melting phase transition, as measured by the $\Delta T_{1/2}$ parameter, increases more or less linearly in each case, this effect is greatest for L_{24}, intermediate for W-L_{22}-W, and smallest for L_{24}-DAP. The possible molecular basis for this effect will also be discussed below.

Fourier Transform Infrared Spectroscopy Studies of Peptide-Containing PC Bilayers. In these studies, infrared spectra of mixtures of the peptide with each of the four PCs studied were recorded as a function of temperature and as a function of the mole fraction of the peptide. The use of FTIR spectroscopy permits a noninvasive monitoring of both the structural organization of the lipid bilayer and the conformation of the incorporated peptide. Thus the gel/liquid-crystalline phase transitions of the lipid bilayer and changes in the degree of rotational isomeric disorder of the lipid hydrocarbon chains can be conveniently monitored by changes in the frequency of the CH_2 symmetric stretching band near 2850 cm^{-1}, changes in solid-state hydrocarbon chain packing by changes in the CH_2 scissoring band near 1468 cm^{-1}, and changes in the hydration and/or polarity of the polar/apolar interfacial region of the lipid bilayer by changes in the contours of the ester carbonyl stretching bands near 1735 cm^{-1}, and changes in peptide secondary structure can be monitored by changes in the conformationally sensitive amide I band near 1650 cm^{-1} (*40*). We find that the incorporation of these peptides into the lipid bilayer does not result in discernible changes in the hydration or the polarity of the polar/apolar interfacial regions of the lipid bilayer but severely inhibits the formation of lipid subgel phases, with the result that, at low temperature, the gel phase frequencies of the CH_2 scissoring band near 1468 cm^{-1} are always typical of rotationally disordered hydrocarbon chains. Thus the only spectroscopic parameters we examined in detail were the amide I band of the peptide and the CH_2 symmetric stretching bands of the phospholipid hydrocarbon chains.

Illustrated in Figure 8 are the temperature-dependent changes in the frequencies of the peptide amide I absorption

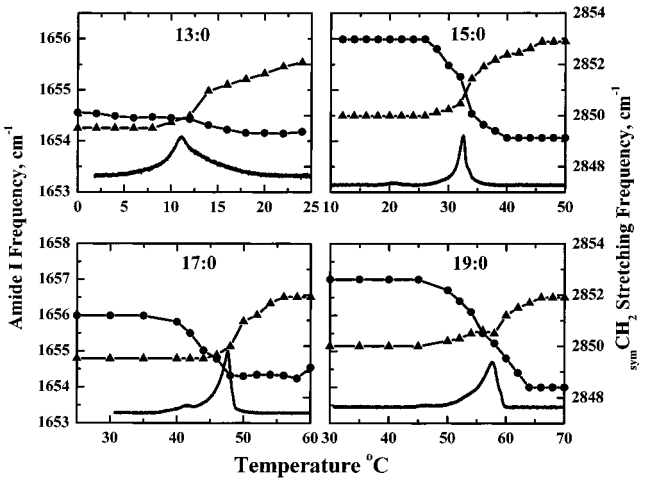

FIGURE 8: Combined plots of CH_2 symmetric stretch (▲), peptide amide I band (●), and DSC thermograms as a function of temperature for systems of L_{24}/13:0, 15:0, 17:0, and 19:0 PC. The peptide concentration is 3.3 mol %.

band and the CH_2 symmetric stretching band of the lipid hydrocarbon chains exhibited by mixtures of L_{24} (3.3 mol %) and each of the four PC studied here. The DSC heating endotherms of each sample are also shown to facilitate a comparison of the calorimetric and FTIR spectroscopic results. In all cases the DSC endotherms are accompanied by an increase in the CH_2 symmetric stretching frequency, indicating that both the sharp and broad components of the DSC endotherms are associated with lipid hydrocarbon chain-melting events (see ref *40*). Moreover, the lipid phase transition is accompanied by a decrease in the frequency of the L_{24} amide I band, and the magnitude of this frequency change tends to increase with increases in the hydrocarbon chain length of the host PC bilayer. This result is entirely attributable to the fact that the amide I band frequencies observed in gel phase bilayers increase with increases in hydrocarbon chain length, whereas the amide I band frequency in the liquid-crystalline state is essentially independent of bilayer thickness (see Figure 8). Qualitatively similar results were obtained when the peptides L_{24}-DAP and W-L_{22}-W were incorporated into these PC bilayers (data not shown). The pattern of hydrocarbon chain length-dependent changes in amide I frequency at the gel/liquid-crystalline phase transition of these lipid/peptide mixtures is similar to that observed when the peptide P_{24} was incorporated into PC and PE bilayers (*15*, *21*) and has previously been ascribed to small conformational distortions of the peptide helix (see ref *41*).

The data presented in Figure 9 illustrate the relative magnitudes of the amide I frequency changes exhibited by peptides L_{24}, L_{24}-DAP, and W-L_{22}-W at the gel/liquid-crystalline phase transition of 19:0 PC. As noted above, the behavior of each of these peptides is qualitatively similar in that the main phase transition of the host lipid bilayer is accompanied by a decrease in amide I frequency. The magnitude of this frequency shift ($\sim$3 cm^{-1}) is similar for all three peptides, suggesting that peptides L_{24}, L_{24}-DAP, and W-L_{22}-W are all comparably responsive to alterations in the thickness of the host PC bilayer. However, a close inspection of the contours of the amide I bands of these peptides indicates that these shifts in overall band frequency are actually caused by changes in the relative intensities of the

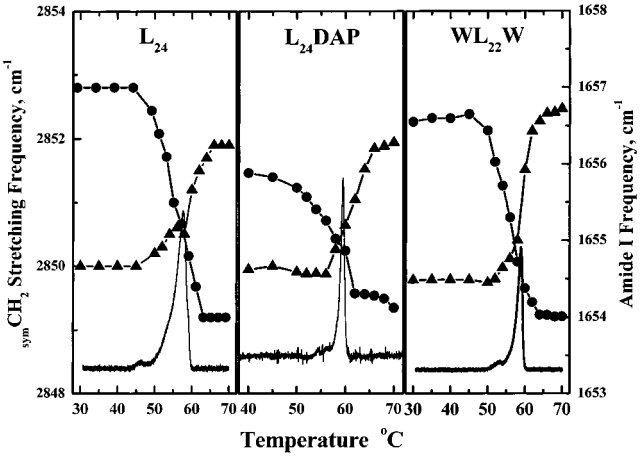

FIGURE 9: Combined plots of CH_2 symmetric stretch (▲), peptide amide I band (●), and calorimetric thermograms as a function of temperature for systems of L_{24}, L_{24}-DAP, W-L_{22}-W, and 19:0 PC. The peptide concentration is 3.3 mol %. Left panel, L_{24}/19:0 PC; middle panel, L_{24}-DAP/19:0 PC; right panel, W-L_{22}-W/19:0 PC.

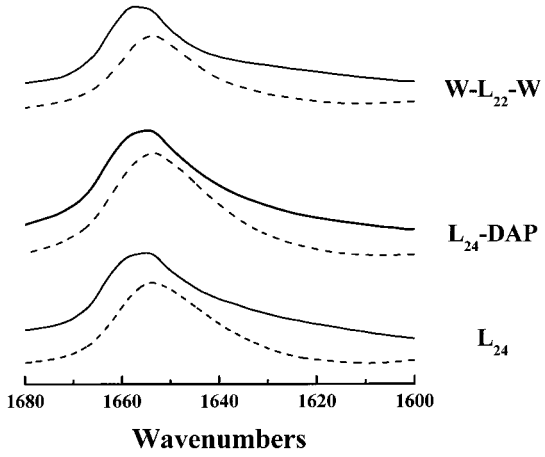

FIGURE 10: Amide I band contours exhibited by peptides L_{24}, L_{24}-DAP, and W-L_{22}-W incorporated into 19:0 PC bilayers. Absorbance spectra are shown for the peptides indicated at temperatures below (solid line) and above (dashed line) the gel/liquid-crystalline phase transition temperatures of the lipid/peptide mixtures. The peptide concentration is 3.3 mol %.

underlying band components (see Figure 10). Specifically, when incorporated into bilayers composed of the longer chain PCs, the amide I absorption bands of all three peptides consist primarily of two components centered near 1653 and 1658−1660 cm^{-1} when the lipids are in the gel state (see Figure 10). Moreover, the lower frequency component exhibited by peptides L_{24} and L_{24}-DAP is relatively more prominent whereas with peptide W-L_{22}-W, the higher frequency component is the more prominent (see Figure 10). We also find that both the intensity and center of gravity of the higher frequency component increase slightly as the thickness of the host bilayer increases in the gel state. However, at temperatures above the lipid gel/liquid-crystalline phase transition, the intensity of the higher frequency component exhibited by all three peptides decreases relative to that of the lower frequency component, and as a result, the overall frequency of the amide I band maximum decreases. Further examination using difference spectral analysis indicates that, with all three peptides, the relative decline in the intensity of the higher frequency component near 1658−1660 cm^{-1} is accompanied by an overall increase in the intensity of

broader components centered near 1645−1649 cm^{-1} (analyses not shown). The possible molecular basis of those spectroscopic observations will be discussed below.

DISCUSSION

A comparison of the thermotropic phase behavior of PC vesicles containing L_{24} (this study) with those containing the closely related P_{24} (*15*) reveals that, in general, these peptides have very similar effects on the organization of their host PC bilayers. With both peptides, DSC thermograms observed at low peptide concentrations can be resolved into two components which are probably attributable to the melting of peptide-poor (sharp component) and peptide-rich (broad component) lipid domains. Moreover, the effects of these peptides on the temperature, enthalpy, and overall cooperativity of the lipid hydrocarbon chain-melting phase transition, the sensitivity of these parameters to the variations in lipid hydrocarbon chain length, the apparent stoichiometry of the peptide/PC interactions, and the magnitude of the hydrophobic mismatch effects observed with these two peptides are essentially the same, within experimental error. Finally, both peptides also exhibit similar patterns of lipid phase state-dependent and lipid hydrocarbon chain length-dependent changes in amide I band frequency when incorporated into PC bilayers. These results provide strong evidence that the spacer amino acid residues Gly-3 and Ala-30 of P_{24} have no significant effect on its interaction with PC bilayers. We therefore conclude that the results of previous extensive studies of P_{24}/phospholipid interactions can be applied with reasonable confidence to the compositionally similar, second generation peptide L_{24}.

Previous FTIR spectroscopic studies have shown that the gel/liquid-crystalline phase transitions of P_{24}/phospholipid mixtures are accompanied by small phase state-dependent amide I frequency shifts (*15*, *16*). Similar studies of $(LA)_{12}$/phospholipid mixtures revealed a more complex phase state-dependent behavior in which the main amide I band of $(LA)_{12}$ appears to be a single component (∼1654 cm^{-1}) in the liquid-crystalline state and a partially resolved summation of two components (∼1665 and 1655 cm^{-1}) when the peptide is dispersed in the gel phases of PE and longer chain PC bilayers (*25*, *26*). Here, we have also revealed a pattern of phase state-dependent amide I frequency shifts which appear to be of comparable magnitude to those observed in previous studies of P_{24}/phospholipid interactions. However, we also find that, when dispersed in the gel phases of the longer chain PCs, the main amide I bands exhibited by L_{24}, L_{24}-DAP, and W-L_{22}-W each contain components centered near 1657−1659 cm^{-1} and near 1653−1654 cm^{-1}, and as previously observed in our studies of $(LA)_{12}$, the intensity of the higher frequency component decreases when the host lipid bilayer converts to the liquid-crystalline state. We also find that the decrease in intensity of the higher frequency component of the amide I band is accompanied by an increase in the intensity of the broader, less well-defined components centered between 1645 and 1649 cm^{-1}. Interestingly, a reexamination of our FTIR spectroscopic data on the interactions of peptides P_{24} and $(LA)_{12}$ with phospholipid bilayers indicates that a similar process was also occurring in those systems, albeit of different magnitude. It is therefore possible that the phase state-dependent amide I frequency shifts reported here and in our previous studies of P_{24} (*15*, *16*) and $(LA)_{12}$ (*25*, *26*) may actually be manifestations of the same physical phenomenon.

In considering the possible physical basis of these FTIR spectroscopic results, we note that the amide I frequencies observed are all in a range consistent with the predominance of α-helical structures, and it is therefore unlikely that our experimental observations are the result of conformational interconversions between α-helical and non-α-helical forms of these peptides. This conclusion is consistent with those made in our previous studies, wherein we suggested that the observed frequency shifts were the result of small alterations in the pitch of the peptide α-helix in response to changes in lipid bilayer thickness (see ref *41*). We also note that amide I frequencies near 1655 cm^{-1} are typical of α-helices with fully protonated peptide amide bonds, whereas amide I frequencies near 1645−1650 cm^{-1} are usually observed when those bonds are fully deuterium exchanged (*42*−*44*). Moreover, the major amide I component near 1653 cm^{-1} is relatively insensitive to changes in lipid phase state and/or lipid bilayer thickness. This observation suggests that most of the amide bonds of these peptides are protected from H−D exchange and are not involved in the structural changes induced by the changes in the phase state or thickness of the host lipid bilayer. Given these observations, the fact that interconversion between amide I components absorbing near 1658−1665 cm^{-1} and a deuterium-exchanged population near 1645−1649 cm^{-1} seems to constitute the basis of the frequency shifts reported here and in our previous studies (*15*, *16*, *25*, *26*), and the fact that the deuterium-exchanged populations of amide bonds are probably localized near the N- and C-termini of these peptides (*45*, *46*), we suggest that the conformational changes which give rise to the higher frequency components observed when these peptides are incorporated into the gel phases of PE and longer chain PC bilayers occur predominantly in the terminal, deuterium-exchanged portions of the peptide α-helix. By comparing the ratios of the integrated intensities of the amide II and amide I absorption bands (for details see ref 24), we estimate that the deuterium-exchanged portion of these peptides accounts for no more than 30% of the total amide protons present (i.e., ≅8 amino acid residues of the 28 amino acid residues present). That the phase state- and bilayer thickness-induced distortions of the α-helical structures of these peptides may actually be limited to their terminal regions is consistent with the inherent stability of their polyleucine cores and with the fraying of the ends of protein and peptide helices. The fact that the higher frequency component predominates in thicker gel-state bilayers, where the thickness of the PC bilayer exceeds the length of the incorporated peptide, is consistent with a stretching of the α-helix to minimize mismatch with host lipid bilayer. Similarly, the fact that the lower frequency component predominates in thinner gel or liquid-crystalline bilayers is consistent with both a reduced stabilization of α-helical structure due to the projection of the peptide termini beyond the conformationally stabilizing bilayer surface and with a greater exposure of the ends of these α-helices to the aqueous phase. However, it will be necessary to confirm these suggestions experimentally, perhaps by using transmembrane peptides with specifically labeled amino acid residues near the chain termini. We note again here that the hydrocarbon chains of the host phospholipid bilayer also alter their conformations to mini-

mize hydrophobic mismatch with the incorporated peptide (*15*, *21*, *34*).

It is interesting to compare the observed effects of the incorporation of L_{24} and L_{24}-DAP on the relative thermal stabilities of the gel and liquid-crystalline states of PC bilayers of different hydrocarbon chain lengths with the effects predicted by the snorkel model (*28*, *29*). According to this model, the four methylene groups separating the terminal amino groups of the side chains of the two Lys residues from the α-carbon atoms should provide considerable flexibility to these residues, allowing L_{24} to better accommodate to any mismatch between the length of the incorporated peptide and the thickness of the host PC bilayer. In contrast, the truncated side chains of the two DAP residues at the ends of L_{24}-DAP should markedly reduce their flexibility and thus their ability to adjust to such mismatches. If one also assumes that the terminal amino groups of the Lys or DAP residues prefer to be located at the level of the polar and negatively charged phosphate group of the PC molecules, where favorable electrostatic and hydrogen-bonding interactions are maximized, and neglecting other effects of this structural modification (see below), the following predictions can be made. In the relatively thin gel-state bilayers formed by 13:0 PC, the two Lys or DAP residues at each end of L_{24} and L_{24}-DAP, respectively, should be located at approximately the same level as the PC headgroups. In this case, these residues should interact with the PC phosphate group in a fairly strong and similar manner, since a snorkeling of the Lys and DAP residue side chains is not required in this case. In contrast, in the relatively very thin liquid-crystalline bilayers formed by 13:0 PC, the two terminal Lys or DAP residues of L_{24} and L_{24}-DAP will be located about 3.5 and 10 Å above the level of the PC polar headgroups, thus projecting into the aqueous phase. Thus, in this case, one predicts that the snorkeling of the Lys but not the DAP residues should permit L_{24} but not L_{24}-DAP to interact more favorably with the PC phosphate groups, differentially stabilizing the liquid-crystalline phase and resulting in a more pronounced decrease in the phase transition temperature in 13:0 PC bilayers containing L_{24} than L_{24}-DAP. Moreover, this result should also be the case even if these peptides tilt to minimize the mismatch between peptide length and bilayer thickness, since snorkeling of the Lys side chains of L_{24} should reduce the degree of peptide tilting required, which is energetically costly as it produces disorder in the host phospholipid bilayer (*47*, *48*). In contrast, in the relatively much thicker gel-state bilayers formed by 17:0 PC, the terminal amino groups of the Lys and DAP residues of L_{24} and L_{24}-DAP, respectively, are located about 5.7 and 7.3 Å below the level of the PC polar headgroups, while in the liquid-crystalline state, terminal amino groups are again located at the same level in the bilayer as the lipid phosphate groups. Thus, in this case, snorkeling of the Lys side chains of L_{24} toward the bilayer surface in the gel-state 17:0 PC system should differentially stabilize this state, resulting in a higher phase transition temperature in L_{24}, as compared to L_{24}-DAP-containing 17:0 PC dispersions. Interestingly, in 15:0 PC bilayers, where the terminal amino groups of the Lys and DAP residues are located below the level of the PC polar headgroups in the relatively thicker gel-state bilayers but above the level of the lipid phosphate groups in the thinner liquid-crystalline bilayers by roughly comparable distances, one predicts that snorkeling of the Lys side chains of L_{24} would stabilize both the gel and liquid-crystalline phases of 15:0 PC bilayers, thus producing no net shift in the lipid phase transition temperature as compared to L_{24}-DAP, a result which is in fact observed experimentally (see Figure 4). However, according to the snorkel hypothesis, the major effect of the increased ability of L_{24} as compared to L_{24}-DAP to accommodate to differences between peptide length and phospholipid bilayer thickness should be that the magnitude of the phase transition temperature shifts as a function of host bilayer thickness should be smaller in the former as compared to the latter peptide. However, the experimental result (see Figure 4) is in fact the opposite of that predicted, suggesting that the snorkeling of the Lys side chains, if it occurs, is not the primary factor in producing the experimentally observed effects of these two peptides on the thermotropic phase behavior of homologous series of PC bilayers examined here. Instead, this result suggests that another effect of the DAP for Lys substitution at the peptide termini must have a greater effect on peptide/phospholipid polar headgroup interactions.

We note that the truncation of the Lys side chain should not only inhibit its ability to alter its depth in the PC bilayer but also weaken the strength of the attractive electrostatic and hydrogen-bonding interactions between the positively charged amino group of the peptide and the negatively charged phosphate group of the phospholipid molecule by increasing the distance between these moieties in the lipid bilayer, even if these two groups reside in the same plane. This is because the longer side chain of the Lys residue results in its terminal amino group projecting beyond the cylindrical surface formed by the polyLeu core of the peptide, permitting interaction with adjacent PC molecules, whereas this is not the case with the much shorter DAP residues. Due to the stronger attractive peptide/phospholipid polar headgroup interactions in PC bilayers generally, one would predict that PC bilayers, in either the L_{α} or L_{β} state, would be differentially stabilized by L_{24} relative to L_{24}-DAP even in the absence of hydrophobic mismatch. Thus in this case one predicts that L_{24} preferentially stabilizes the gel phase in 13:0 PC bilayers and the liquid-crystalline state in 17:0 PC bilayers, thus producing a steeper dependence of the phase transition temperature on PC hydrocarbon chain length in L_{24}-containing as compared to L_{24}-DAP-containing systems. In fact, this is what is observed experimentally (see Figure 4), suggesting that the length per se, rather than the flexibility, of the side chains of the positively charged terminal amino acid residues may be of more importance for the interactions of these peptides with the polar headgroups of the phospholipid molecules of the host bilayer. Moreover, we would predict that this latter effect would be even more prominent in anionic as compared to zwitterionic phospholipid bilayers, a hypothesis currently being tested. We note here, however, that in all other respects L_{24} and L_{24}-DAP behave essentially identically when incorporated in PC bilayers of varying thickness. Thus the substitution of DAP for Lys residues has only minor effects on the overall organization of the host PC bilayer.

A comparison of the observed and predicted effects of the incorporation of L_{24} and W-L_{22}-W on the relative thermal stabilities of the gel and liquid-crystalline states of bilayers composed of PCs with different hydrocarbon chains can also

be made. As discussed earlier, aromatic residues in general, and Trp and Tyr residues in particular, tend to occur near the ends of the α-helical transmembrane segments of membrane proteins, being located in the so-called flanking regions between the hydrophobic central region and the charged amino acids which often terminate the α-helical segment (*30*−*32*). These aromatic residues are thus located in the region of the glycerol backbone of the phospholipid molecules composing the host bilayer, between the polar headgroup and the nonpolar hydrocarbon chains (*30*−*32*). It has been suggested that Trp and Tyr residues are particularly well suited to reside in this region of intermediate polarity of the phospholipid bilayer, most likely because their rigidity and flat shape limit access to the hydrocarbon core and the π electronic structure and aromaticity favor residing in an electrostatically complex interfacial environment (*49*−*51*).

If we assume that Trp residues are better suited to localization near the glycerol backbone region of the phospholipid molecules than are Leu residues, we can then predict what the relative effect of L_{24} and W-L_{22}-W would be on the gel/liquid-crystalline phase transition temperature of PC bilayers of different thicknesses, using the rationale presented above for the comparison of L_{24} and L_{24}-DAP. In particular, we predict that mixtures of W-L_{22}-W and PC bilayers where the length of the peptide and the thickness of the host phospholipid bilayer are well matched should be differentially stabilized relative to the same system containing comparable amounts of L_{24}. Thus W-L_{22}-W should differentially stabilize the gel phase of bilayers composed of 13:0 PC and the liquid-crystalline phase of bilayers composed of 17:0 PC, as mismatch between the location of the Trp residues of the peptide and the glycerol backbone regions of the host lipid bilayer is minimized in these systems. As well, in thinner PC bilayers, the possible exposure of the more polar and positively charged Trp residues to the phospholipid polar headgroups and to the aqueous phase is probably less energetically costly than is the exposure of the uncharged and hydrophobic Leu residues. Moreover, in thicker PC bilayers, the energetic cost of inserting the Trp residues of W-L_{22}-W into the hydrophobic core of the lipid bilayers should be greater than that for inserting the Leu residues of L_{24}. These two effects should produce a greater dependence of the peptide-induced shifts in the gel/liquid-crystalline phase transition on the hydrocarbon chain length of the PC molecules for W-L_{22}-W than for L_{24}. However, the opposite result is observed experimentally (see Figure 4). Again, we conclude that effects of the Trp for Leu substitution, other than the relative affinities of these amino acid residues for the glycerol backbone region of the PC molecule, must have a greater influence on peptide/lipid interactions in these systems.

In closing, we wish to emphasize that our results should not be interpreted as indicating that the possible snorkeling of the Lys side chains and the affinity of Trp residues for the polar/nonpolar region of the host phospholipid bilayer are not important for the structure and function of natural transmembrane proteins or for the accommodation of such proteins to environmentally induced variations in the thickness of the host lipid bilayer. In this regard we note that the focus of the present study is on the perturbation of the thermotropic phase behavior of bilayers composed of PCs of different hydrocarbon chain length, which can in principle be affected by a variety of physical properties of the peptide analogues examined here. Moreover, the strong affinity of the polyleucine core of L_{24} and its analogues for the hydrophobic core of the host lipid bilayer may have partially obscured the effects of amino acid substitutions near the peptide terminus. Certainly the work of Killian et al. (*52*−*54*) on Leu-Ala-based transmembrane peptides has demonstrated differential effects on Lys- and Trp-capped peptides on phospholipid thermotropic phase behavior and organization. Nevertheless, it is noteworthy that the incorporation of L_{24}, L_{24}-DAP, and W-L_{22}-W has such generally similar effects on the thermotropic phase behavior of these PC bilayers.

REFERENCES

1. Gennis, R. B. (1989) in *Biomembranes: Molecular Structure and Function*, Springer-Verlag, New York.
2. Yeagle, P. (1992) in *The Structure of Biological Membranes*, CRC Press, Boca Raton, FL.
3. Sandermann, H. (1978) *Biochim. Biophys. Acta 515*, 209−237.
4. McElhaney, R. N. (1982) in *Current Topics in Membranes and Transport* (Razin, S., and Rottem, S., Eds.) Vol. 17, pp 317−380, Academic Press, New York.
5. McElhaney, R. N. (1985) in *Membrane Fluidity in Biology* (Alora, R. A., and Boggs, J. M., Eds.) Vol. 4, pp 147−208, Academic Press, New York.
6. McElhaney, R. N. (1986) *Biochim. Biophys. Acta 864*, 361−421.
7. Watts, A., and De Pont, J. J. H. H. M., Eds. (1985) *Progress in Lipid−Protein Interactions*, Vol. 1, Elsevier, Amsterdam.
8. Watts, A., and De Pont, J. J. H. H. M., Eds. (1986) *Progress in Lipid−Protein Interactions*, Vol. 2, Elsevier, Amsterdam.
9. Marsh, D., and Horváth, L. I. (1998) *Biochim. Biophys. Acta 1376*, 267−296.
10. Watts, A. (1998) *Biochim. Biophys. Acta 1376*, 297−318.
11. White, S. H., and Wimley, W. C. (1998) *Biochim. Biophys. Acta 1376*, 339−352.
12. Killian, J. A. (1998) *Biochim. Biophys. Acta 1376*, 401−416.
13. Davis, J. M., Clare, J. M., Hodges, R. S., and Bloom, M. (1983) *Biochemistry 22*, 5298−5305.
14. Zhang, Y.-P., Lewis, R. N. A. H., Hodges, R. S., and McElhaney, R. N. (1992) *Biochemistry 31*, 11572−11578.
15. Zhang, Y.-P., Lewis, R. N. A. H., Hodges, R. S., and McElhaney, R. N. (1992) *Biochemistry 31*, 11579−11588.
16. Axelsen, P. H., Kaufman, P. H., McElhaney, R. N., and Lewis, R. N. A. H. (1995) *Biophys. J. 69*, 2770−2781.
17. Huschilt, J. C., Millman, B. M., and Davis, J. H. (1989) *Biochim. Biophys. Acta 97*9, 139−141.
18. Bolen, E. J., and Holloway, P. W. (1990) *Biochemistry 29*, 9638−9643.
19. Huschilt, J. C., Hodges, R. S., and Davis, J. H. (1985) *Biochemistry 24*, 1377−1386.
20. Morrow, M. R., Huschilt, J. C., and Davis, J. H. (1985) *Biochemistry 24*, 5396−5406.
21. Zhang, Y.-P., Lewis, R. N. A. H., Hodges, R. S., and McElhaney, R. N. (1995) *Biophys. J. 68*, 847−857.
22. Pauls, K. P., MacKay, A. L., Soderman, O., Bloom, M., Taneja, A. K., and Hodges, R. S. (1985) *Eur. Biophys. J. 12*, 1−11.
23. Subczynski, W. K., Lewis, R. N. A. H., McElhaney, R. N., Hodges, R. S., Hyde, J. S., and Kusumi, A. (1998) *Biochemistry 37*, 3156−3164.
24. Zhang, Y.-P., Lewis, R. N. A. H., Henry, G. D., Sykes, B. D., Hodges, R. S., and McElhaney, R. N. (1995) *Biochemistry 34*, 2348−2361.
25. Zhang, Y.-P., Lewis, R. N. A. H., Hodges, R. S., and McElhaney, R. N. (1995) *Biochemistry 34*, 2362−2371.
26. Zhang, Y.-P., Lewis, R. N. A. H., Hodges, R. S., and McElhaney, R. N. (2001) *Biochemistry 40*, 474−482.
27. Lewis, R. N. A. H., Zhang, Y.-P., Hodges, R. S., Subczynski, W. K., Kusumi, A., Flach, C. R., Mendelsohn, R., and McElhaney, R. N. (2001) *Biochemistry 40*, 12103−12111.
28. Segrest, J. P., De Loof, H., Dohlman, J. G., Brouillette, C. G., and Anantharamaiah, G. M. (1990) *Proteins: Struct., Funct., Genet. 8*, 103−117.

29. Monne, M., Nilsson, I., Johansson, M., Elmhed, N., and van Heijne, G. (1998) *J. Mol. Biol. 284*, 1177−1183.
30. Von Heijne, G. (1999) *Q. Rev. Biophys. 32*, 285−307.
31. Popot, J.-L., and Engelman, D. M. (2000) *Annu. Rev. Biochem. 69*, 881−992.
32. Jayasinghe, S., Hristova, K., and White, S. H. (2001) *Protein Sci. 10*, 455−458.
33. Mantsch, H. H., Madec, C., Lewis, R. N. A. H., and McElhaney, R. N. (1985) *Biochemistry 24*, 2440−2446.
34. Pare, C., Lafleur, M., Liu, F., Lewis, R. N. A. H., and McElhaney, R. N. (2001) *Biochim. Biophys. Acta 1511*, 60−73.
35. Morrow, M. R., Huschilt, J. C., and Davis, J. H. (1985) *Biochemistry 24*, 5396−5406.
36. Lewis, R. N. A. H., Mak, N., and McElhaney, R. N. (1987) *Biochemistry 26*, 6118−6126.
37. Owicki, J. C., and McConnell, H. M. (1979) *Proc. Natl. Acad. Sci. U.S.A. 76*, 4750−4754.
38. Mouritsen, O. G., and Bloom, M. (1984) *Biophys. J. 46*, 141−153.
39. Riegler, J., and Mohwald, H. (1986) *Biophys. J. 49*, 1111−1118.
40. Lewis, R. N. A. H., and McElhaney, R. N. (1996) in *Infrared Spectroscopy of Biomolecule*s (Mantsch, H. H., and Chapman, D., Eds.) pp 159−202, John Wiley and Sons, New York.
41. Chirgadze, Y. N., Brazhnikov, E. V., and Nevskaya, N. A. (1976) *J. Mol. Biol. 102*, 781−792.
42. Chirgadze, Y. N., and Brazhnikov, E. V. (1974) *Biopolymers 13*, 1701−1712.
43. Rabolt, J. F., Moore, W. H., and Krimm, S. (1977) *Macromolecules 10*, 1065−1074.
44. Dwivedi, A. M., and Krimm, S. (1984) *Biopolymers 23*, 923−943.
45. Nakanishi, M., Tsuobi, M., Ikegami, A., and Kanehisa, M. (1972), *J. Mol. Biol. 64*, 363−378.
46. Dempsey, C. E. (1988) *Biochemistry 27*, 6893−6901.
47. Li, L. (2000) *Biophys. Chem. 86*, 79−83.
48. Harzer, U., and Bechinger, B. (2000) *Biochemistry 39*, 13106−13114.
49. Yau, W. M., Wimley, W. C., Gawrisch, K., and White, S. H. (1998) *Biochemistry 37*, 14713−14718.
50. Persson, S., Killian, J. A., and Lindblom, G. (1998) *Biophys. J. 75*, 1365−1371.
51. White, S. H., and Wimley, W. C. (1999) *Annu. Rev. Biophys. Biomol. Struct. 28*, 319−365.
52. Killian, J. A., Salemink, I., de Planque, M. R. R., Lindblom, G., Koeppe, R. E., and Greathouse, D. V. (1996) *Biochemistry 35*, 1037−1045.
53. de Planque, M. R. R., Greathouse, D. V., Koeppe, R. E., Schafer, H., Marsh, D., and Killian, J. A. (1998) *Biochemistry 37*, 9333−9345.
54. de Planque, M. R. R., Kruijtzer, J. A. W., Liskamp, R. M. J., Marsh, D., Greathouse, D. V., Koeppe, R. E., de Kruijff, B., and Killian, J. A. (1999) *J. Biol. Chem. 274*, 20839−20846.

BI025661I